Shape Decision of High Energy Density Beam†

Yoshiaki ARATA*, Michio TOMIE**, Kiyoshi TERAI***, Hiroyoshi NAGAI*** and Tetsuji HATTORI***

Abstract

A new principle and device of measuring accurate beam shape, focal point and energy density of a beam was proposed by using the same beam (beam voltage, beam current, welding speed, gas pressure in vacuum chamber and a_b value) as used in the practical welding.

This method can be applied to any high power and high energy density beam and to all the weldable materials. The authors recommended stainless steel, killed steel or ceramics as a testing material which gives superior quality obtaining beam diameter and is convensional material. With application of this method, the interaction between electron beam and its beam plasma becomes strong around the vacuum of $(0.3-1)\times10^{-1}$ Torr, and phenomena of expanding beam diameter ("beam expansion") and marked decrease of energy density of beam were obviously observed.

1. Introduction

In the high energy density beam welding such as electron beam and laser beam welding, there appears a parameter which represents the location of the beam focal point for a workpiece besides beam voltage, beam current and welding speed as the fundamental welding parameter. This parameter, a_b value, acts as an important factor in giving considerable effects on penetration depth, width of bead, shape of bead and appearance of weld defects, and the definition and characteristics of which have reported in detail by Arata and co-workers[1)~5)]. As shown in **Fig. 1,** the beam zone in the vicinity of focal point beam

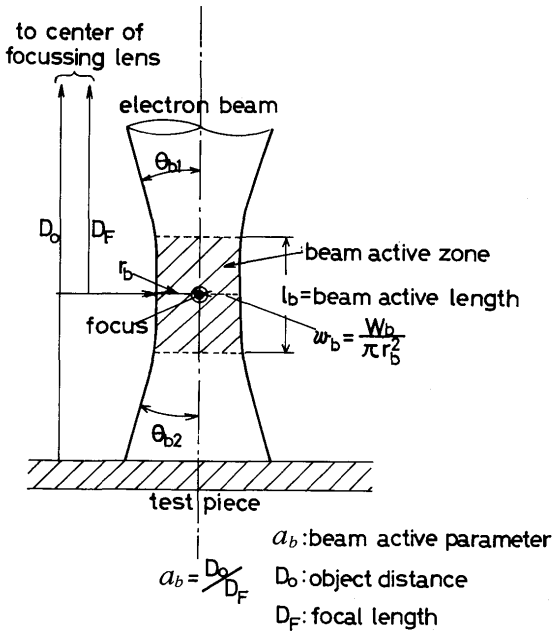

Fig. 1. Schematic diagram illustrated both shape of electron beam and beam parameters.

active zone, having high energy density gives a shape of bead that shows the most remarkable characteristics of this welding method featuring narrow width of bead and deep and sharp penetration. On the contrary, however, it easily gives rise to such weld defects as porosity, spike and cold shut. While, the beam zone off around the focal point gives a shape of bead having wide width of bead and relatively shallow penetration depth that serves to prevent those weld defects.

In order to clarify these fundamental phenomena and mechanism of bead penetration, it should be required to know the accurate beam shape, that is, beam diameters varied continuously in relation to the distance from the focusing coil and its energy density particularly those at the focal point.

Despite various methods have been tried, no satisfactory method is yet being established due to its extreme difficulty in measuring the shape of beam having high power and high energy density as used in practical welding process, which differs from the measurement of beam diameter having a low power that no melting action is given to the test piece by the irradiation of electron beam as used for the electron microscope. Furthermore, no experiment has so far been tried on the method to determine the shape of beam and focal point during the process of practical welding.

In this technical paper, therefore, the method of measuring the shape of high power and high energy density beam during the practical welding process is proposed and its usability proved by the many experiments, and more the feature of the beam is studied.

† Received on Aug. 3, 1973
* Professor
** Research Associate
*** Welding Research Department, Kawasaki Heavy Industries, Ltd.

2. Preliminary Research

The measuring methods of the shape of beam are largely classified one with melted beam irradiation point and no melted point. For the former, use of sheet material, utilization of burn through phenomenon and use of easily vaporized material are considered as essential means. However, there has been lack of reappearance and reliability in the conventional testing methods and functions of testing materials. For the latter, measurements have been made by the linear or circular movement of the cooling plate or bar[6]. Since application of this method is limited to the range within the low beam power in which the cooling plate is not melted, it is not a suitable method to measure the shape of high power and high energy density beam as used in welding.

In this paper, the authors describe the measuring methods of effective beam diameter for the practical electron beam and its usability is studied through various experiments.

Firstly, effects of various plate thickness on the burn through phenomenon at the weld zone were examined by using the step type workpiece having its thickness from 2 mm to 20 mm ($40^{(W)} \times 240^{(L)}$, 40 mm length for each thickness) as shown in **Fig. 2.** In this

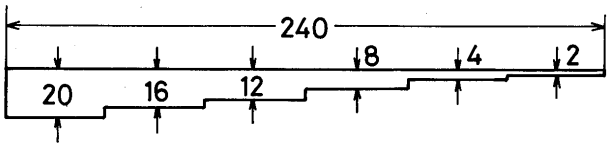

Fig. 2. Step type test piece.

test, effects of welding speed were also examined with the speed varied in four steps as the only parameter. Austenitic stainless steel AISI 304 was used as a test piece, and the bead was given by the electron beam welding machine 150 KV-40 mA type (6 KW). As the result, kerf or "beam groove", moving zone of beam hole where molten metal is not filled up, on both side and its width are shown in **Photo. 1** and **Table 1.**

The conclusion from the facts described above is as follows.

1) Marked variation of kerf or beam groove by plate thickness change despite a value remained unchange.
2) Key hole action as seen in plasma arc welding appears as the plate thickness becomes smaller, molten metal residued without burn through, which resulted in appearance of "secondary melting phenomenon" giving varied kerf or beam groove.
3) This method is considered not practical because a

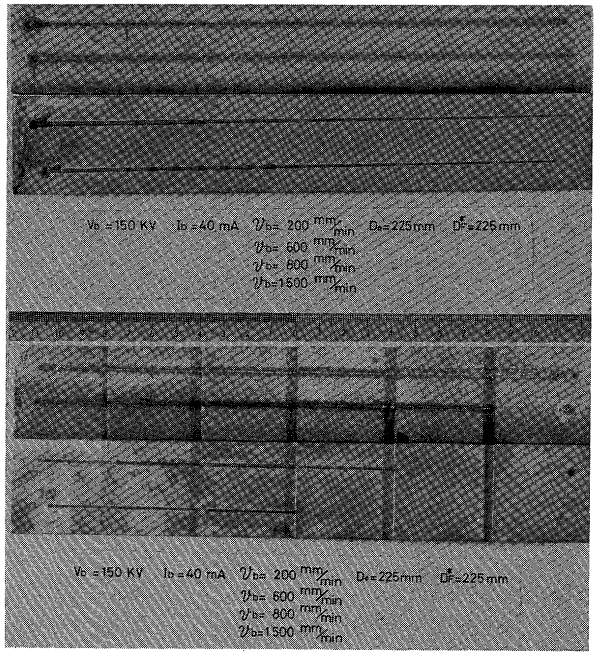

Photo. 1. Surface and reverse bead profile for various welding speed.

Table 1. Bead width for various test piece thickness. (V_b=150 KV, I_b=40 mA, v_b=200 mm/min).

thickness (mm)	20	16	12	8	4	2
bead width (mm)	0.81	1.05	0.88	0.95	1.50	1.70

large number of test pieces is required to observe continuous change of the shape of beam along its axis.

Secondly, "slope welding" method was then applied as shown in **Fig. 3** by using the test piece with much smaller plate thickness for the purpose of clarifing corelation between kerf width and beam diameter when beam cutting was performed, and continuous change of the shape of beam. In this test, stainless steel (AISI 304) with 1 mm plate thickness, nickel with 0.4 mm and monel metal with 0.2 mm were used.

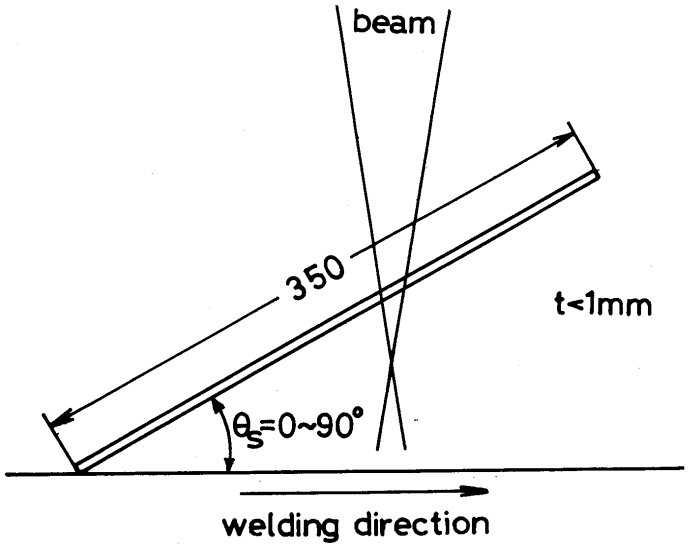

Fig. 3. Schematic drawing of slope welding with thin plate.

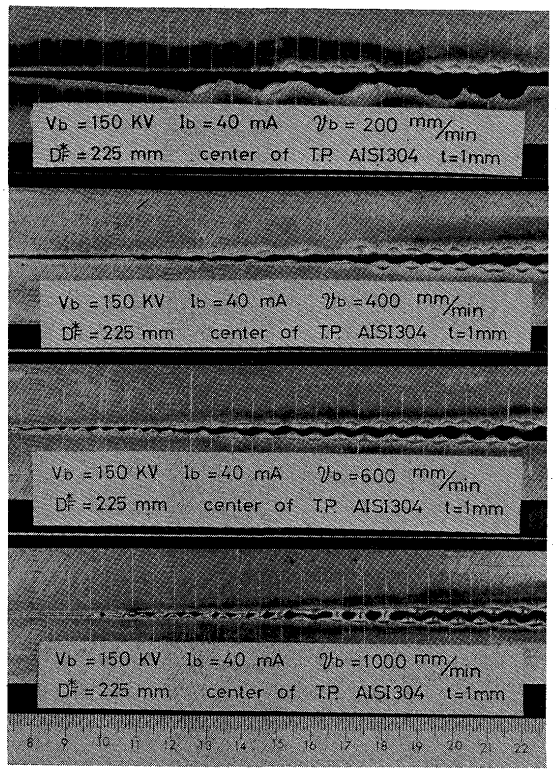

Photo. 2. Secondary melting effect of condensation of molten metal by surface tension for various welding speeds (stainless thin plate).

The results are, as shown in **Photo. 2,** that secondary melting effect of molten metal decreases as welding speed increases, and the kerf width which makes it possible to estimate continuous change of beam diameter can be obtained. On the contrary, adhesion phenomenon of molten metal to the kerf wall by surface tension is further promoted. This phenomenon appears, as shown in **Photo. 3,** even when different materials with much smaller plate thickness are used. This is a substantial phenomenon and cannot be avoided. It has been proved, however,

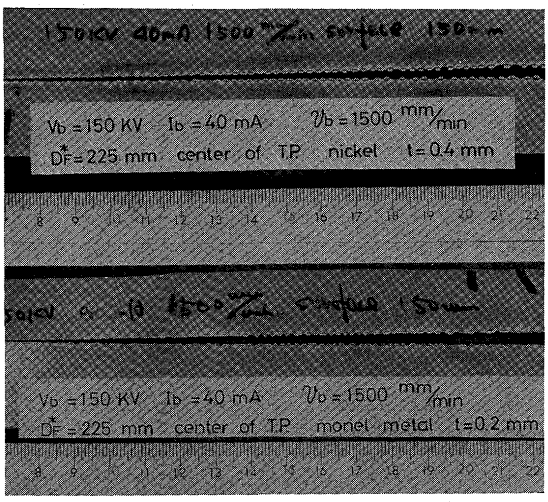

Photo. 3. Condensation of molten metal by surface tension in case of changing plate thickness.

that the slopewelding method used here was extremely effective in observation of the shape of beam at a glance by the use of one test piece.

From the above facts, it has been concluded that the slope welding is the most suitable as a testing method of the shape of beam (simply called "beam test method" or "beam test") which can be observed the shape of beam in a wide range, and for the test piece, it should be necessary to have enough thickness to function rapid and effective removal of molten metal.

Accordingly, the authors have found that such function of the test piece can be given by the application of "edge effect" of a thick plate. Properties of a sharp edge of the thick test piece with profitable angle may be easily estimated as follows.

1) The tip will be vaporized or melted by the slight beam energy.

2) Excess beam energy given around the tip is absorbed rapidly in the base zone, cool and large heat absorber expanding under the tip in the form of heat energy. This action is so powerful that condensation of molten metal by the surface tension will not be allowed to occur, as shown in Photos. 2 and 3.

3) In the case of powerful beam having such excess power that even melts the heat absorber as in welding, most part of the energy is absorbed in the form of melting heat absorber. And at the same time, such melted heat absorber will be removed from the edge zone rapid enough not to occur secondary melting. The authors call such property "edge effect". The test piece with such edge effect therefore is used for the beam test performed by the authors. And, in order to obtain a test piece to put to practical use as well as to meet the purpose, examination was made on edge effects with various shapes and sizes as shown in **Fig. 4.** As a result, test piece with edge shape as shown in **Fig. 5** is selected from more than 10 types of test piece to be used for the beam test methods A type and B type.

A type, as formerly described, is so called "slope welding" using a test piece having slope angle $\theta_s \approx 0° \sim 90°$ which makes one-dimensional movement in horizontal axial direction, and B type is a method

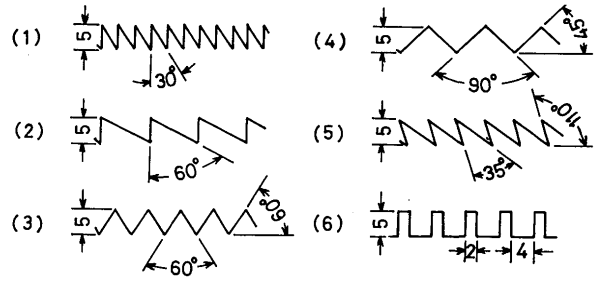

Fig. 4. The kinds of edge shapes.

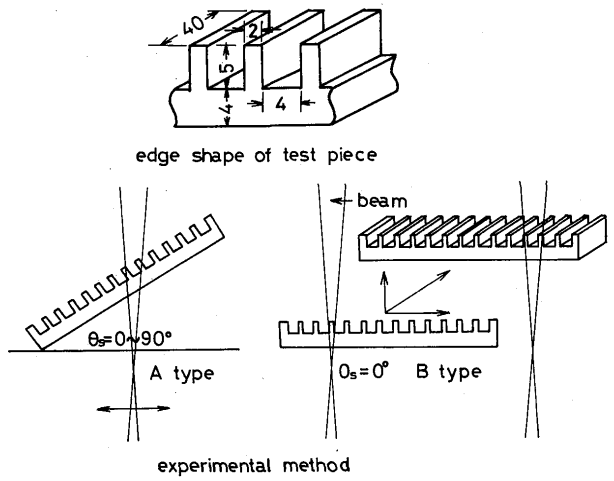

Fig. 5. Schematic drawing of beam test methods.

simply called "glide-welding" by the authors using a test piece having $\theta_s = 0°$ which makes oblique movement (two-dimensional movement) along the gradient with glide angle θ_s.

Fig. 6 is the fundamental drawing of the test device. The slope angle is determined by the length of beam zone to be measured (length of test piece required for the purpose) and the condition of fluid of liquid metal from the molten pool. When beam power becoms large or speed is slow, it is necessary to have small $\theta_s = \pm(15°\sim45°)$ is most frequently used. In this test $\theta_s = \pm 30°$ was used.

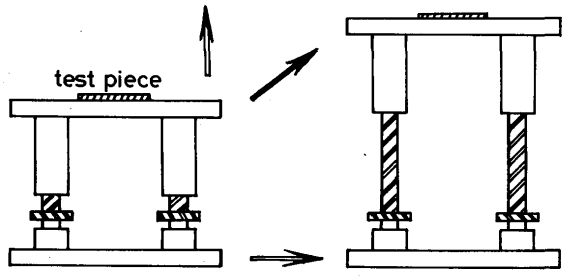

Fig. 6. Schematic drawing of glide beam test method device.

The symbol,+,shows upslope-welding which gives a welding bead going toward upside along a slope with θ_s, and symbol,−, shows downslope-welding which gives a welding bead going toward downside along the same sloping surface. As shown in **Fig. 7,** when $\theta_s = +30°$ the molten metal is rather widened in the vicinity of the most narrowly focussed beam active zone (focal point) compared to that in case of $\theta_s = -30°$. This is because, in case of upslope-welding, liquid metal in the molten pool tends to flow only downward and to gather in the beam groove near the surface. Such tendency becomes more and more conspicuous with larger θ_s and slower welding speed at the narrower beam groove, i. e., near the focal point to occur secondary melting.

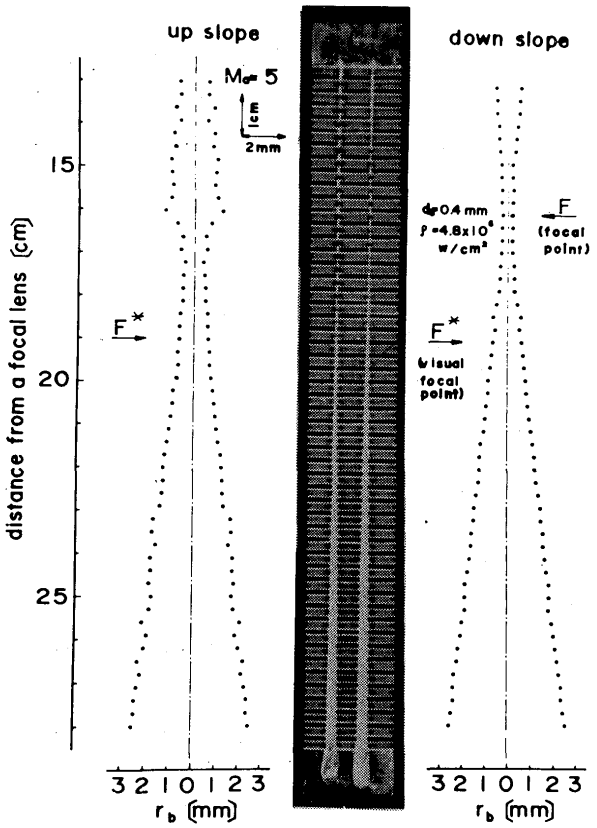

t=8, V_b=150 kV, I_b=40 mA, v_b=60cm/min

Fig. 7. Difference of measured beam shape between up slope welding and down slope welding.

Accordingly, $\theta_s = -30°$ was used for any A type test with edge shape of a test piece as shown in Fig. 5. It is natural that, for B type, no such action needs to be considered because $\theta_s = 0°$.

3. Shape Decision of High Energy Density Beam

3-1 Used materials and test device

Table 2 shows materials and their chemical composition used for test. The test piece has the edge shape shown in Fig. 5 from the results of Preliminary

Table 2. Chemical composition of test piece.

material	mark	chemical composition
stainless steel	AISI 316L	C ≤0.08, Si ≤1.00, Mn ≤2.00, P ≤0.04, S ≤0.03, Ni 12.00~16.00, Cr 16.00~18.00, Mo 2.00~3.00, Fe Bal
phosphor bronze	PBC-1	Sn 10.0~13.0, P 0.05~0.15, Pb+Zn+Fe ≤1.5, Cu Bal
copper	DCuP2 -½	P 0.004~0.040, Cu Bal
titanium	KS-40	C+Fe+N ≤0.60, O ≤0.300, H ≤0.010, Ti Bal
aluminum alloy	5083	Cu ≤0.1, Si ≤0.4, Fe ≤0.4, Mn 0.3~1.0, Mg 3.8~4.8, Zn ≤0.1, Ti ≤0.2, Cr ≤0.5, Al Bal
aluminum alloy	7075	Cu 1.2~2.0, Si ≤0.4, Fe ≤0.5, Mn ≤0.3, Mg 2.1~2.9, Zn 5.1~6.1, Ti ≤0.2, Cr 0.18~0.35, Al Bal

Research with the size $40^{(W)} \times 350^{(L)}$. The welding device is 150 KV-40 mA Hamilton type 6 KW EB welder which has variable gas pressure in vacuum chamber from 10^{-1} Torr to more than 5×10^{-4} Torr.

3-2 Test methods

The test adopts the shape of test piece and beam test methods based on the results of Preliminary Research. For test procedures, firstly austenitic stainless steel AISI 316L was selected as a representive test piece, which was fixed with a jig at slope angle 30° based on Fig. 5 A type test method, and downslope welding was performed to examine effects of various factors (beam voltage: V_b, beam current: I_b, welding speed: v_b, a_b value and gas pressure in vacuum chamber: P_{ch} on the shape of beam. The same method was applied on test piece of titanium, copper and its alloy, alminium alloy to examine effects of materials on the shape of beam.

In order to examine effects of vaporization on the measurement of the shape of beam, A type beam test method was applied by using 7075 Al alloy, in which easily vaporized element (zinc, etc.) is contained, and quartz to measure the shape of beam. Quartz test piece used here was a thin plate having $2\ mm^{(t)} \times 40^{(W)} \times 300^{(L)}$.

A similar test to A type was further performed on AISI 316L steel and titanium based on B type beam test method as shown in Fig. 5 using a device as shown in Fig. 6 to compare with the results of A type test method. Prior to welding, grease was removed from all the test pieces by methyl-ethyl ketone. For the determination of measured value of beam diameter, average of three points, i. e., the measured point, before and behind it, was calculated to be adopted as measured value.

3-3 Test results

3-3-1 Effects of welding factors on the shape of beam

AISI 316L stainless steel was used to examine effects of various welding factors on the shape of beam. **Figs. 8~12** show the results. When burn through region of each edge for the test piece, i. e., its kerf width or beam groove represents the beam diameter, these figures show the changes of such beam diameter by the distance from the focusing lens.

Fig. 8 shows how the beam diameter becomes larger as beam voltage decrease, Fig. 9 shows how the beam diameter becomes larger as beam current increases. These tendencies can easily be predicted when considering velocity of electrons and action of space charge based on the beam current value.

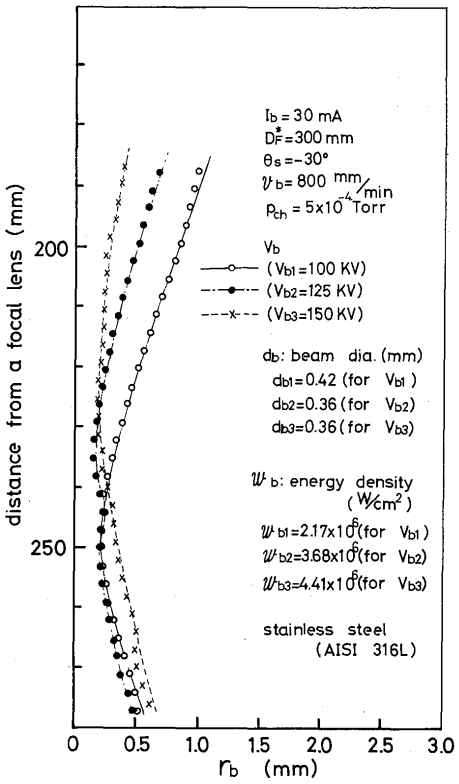

Fig. 8. Relation between beam voltage and beam shape (A type test).

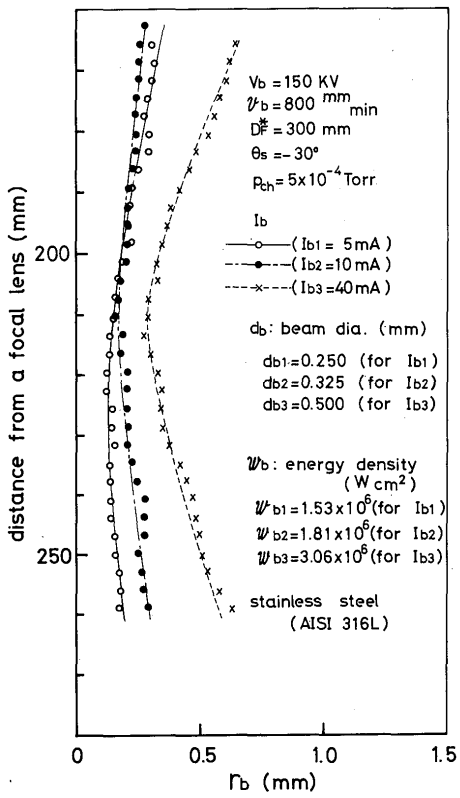

Fig. 9. Relation between beam current and beam shape (A type test).

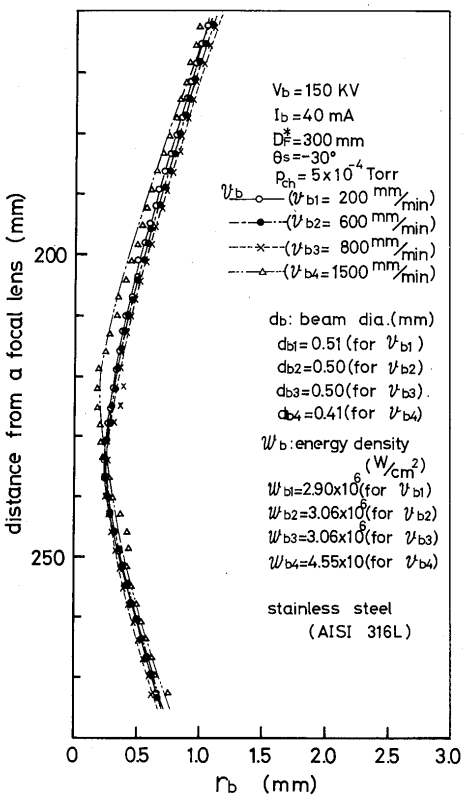

Fig. 10. Relation between welding speed and beam shape (A type test).

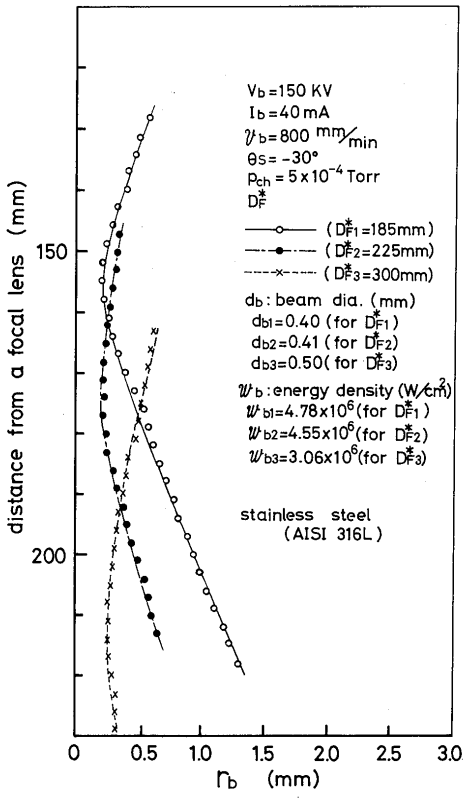

Fig. 11. Relation between visual focal length and beam shape (A type test).

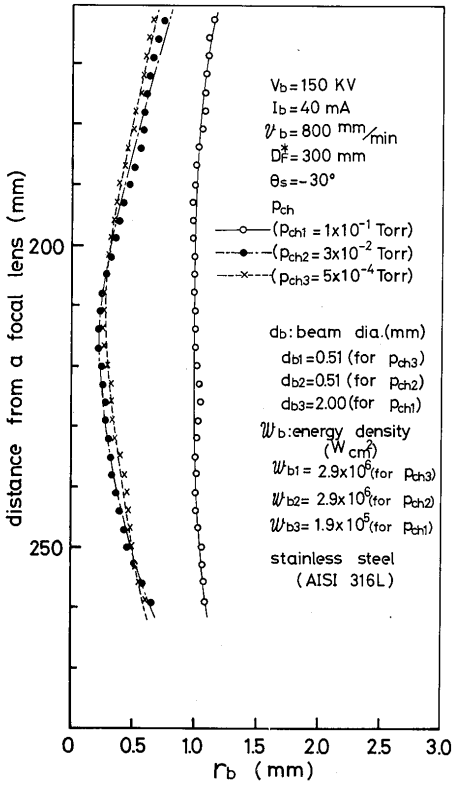

Fig. 12. Relation between gas pressure in vacuum work chamber and beam shape (A type test).

Fig. 10 shows effects of welding speed, which indicates that such change of speed does not give any effect on the shape of beam for AISI 316L stainless steel.

Fig. 11 shows effects of visual focal point on the beam diameter. The visual focal point defines as the target position where beam spot is the smallest, its brightness the highest and is observed visually when the beam of small current (1～2 mA) is irradiated on the target of movable tungsten. The results of Fig. 11 prove that the true focal point of the practical beam welding is located considerably upper from each visual focal point (for example, true focal points for Hamilton type 6 KW electron beam welding machine are located approximately 3 cm, 5 cm, 7.5 cm upper from each visual focal point 18.5 cm, 22.5 cm, 30.0 cm.). Since these facts play extremely important role, true focal point of the welding beam by the beam power must be measured prior to practical welding.

The minimum beam diameter tends to be widened slightly as visual focal point becomes longer.

Fig. 13 shows relation between visual focal point D^*_F, penetration depth h_p and object distance D_o (distance from focusing coil to test piece). Such relation is more clearly expressed by visual beam active

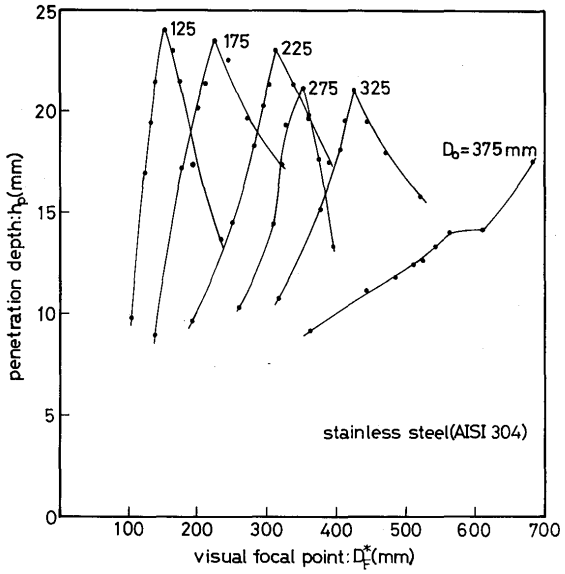

Fig. 13. Relation between penetration depth and visual focal point for various object distance, (V_b=150 KV, I_b=30 mA, v_b=500 mm/min.).

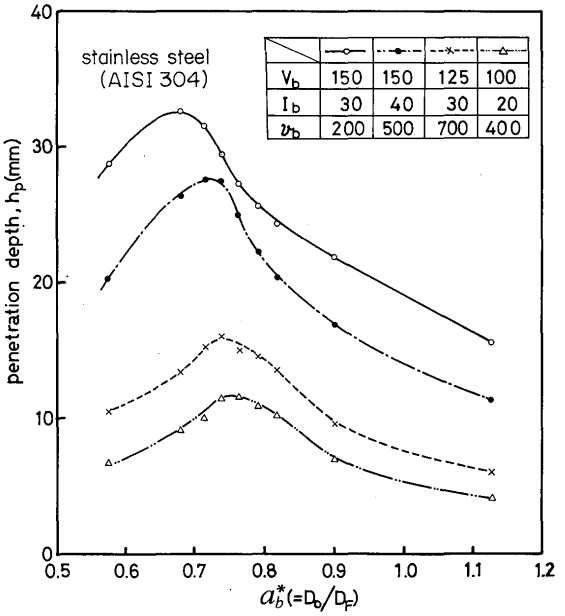

Fig. 14. Relation between penetration depth and visual active parameter: a_b^* .

parameter a_b^* ($\equiv D_o/D^*_F$) as shown in **Fig. 14.** The object distance at the visual focal distance corresponding to each maximum penetration depth as shown in Fig. 13, is located near the real focal distance obtained from Fig. 11 under same visual focal distance above mentioned, which can be easily explained in consideration of its energy density[7]. From these facts described above, penetration depth reaches the maximum when focal point comes near the immediate below the test piece surface as shown in **Fig. 15.**

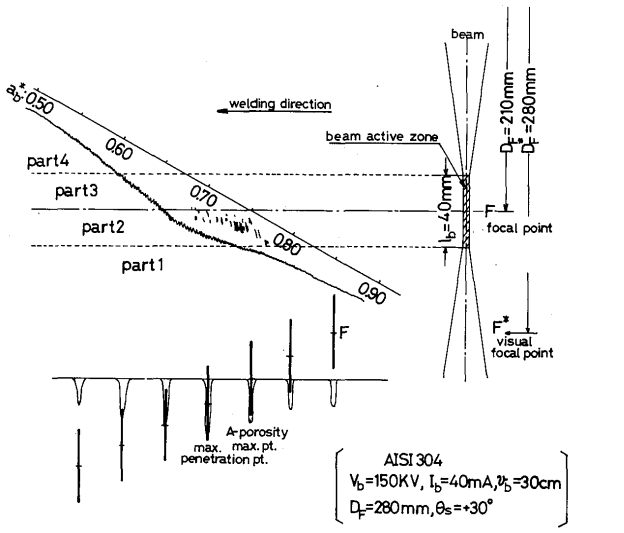

Fig. 15. Schematic explanation of mutual relation on situation between occuring range of porosity. and beam.

Fig. 12 shows effects of gas pressure in vacuum work chamber, P_{ch} on the beam diameter. It seems that the beam diameter measured vacuum chamber having gas pressure from high vacuum condition to 3×10^{-2} Torr receives so little effect of P_{ch} that is can be disregarded. The beam diameter rather looks slightly smaller around 10^{-2} Torr than high vacuum is considered may be due to the action of plasma lens force. When the degree of vacuum lowers to 1×10^{-1} Torr, it is observed that the beam diameter suddenly widened largely. This suggests that interaction between electron beam and its beam plasma becomes abruptly strong in the vacuum range of $(0.3-1)\times10^{-1}$ Torr, and change in mechanism of collision. Such vacuum range is called "beam expansion vacuum". This new fact has obviously discovered for the first time by A type beam test device, which indicates abrupt decrease of the beam energy density in this vacuum range. It is considered that the above fact will give extremely important contribution to understanding and application of welding phenomenon. For example, well known relation between gas pressure in vacuum chamber and penetration depth as shown in **Fig. 16** is remarkably well explained[7].

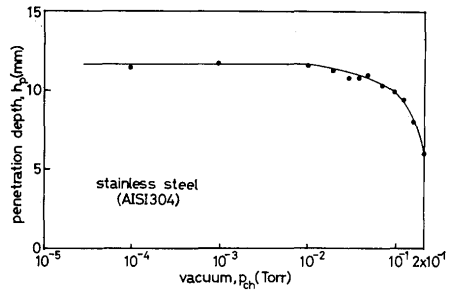

Fig. 16. Relation between penetration depth and gas pressure in vacuum work chamber.

3-3-2 Effects of variation in material on the shape of beam

The same method as that for AISI 316L stainless steel was applied to titanium, copper, phosphor bronze and 5083 Al alloy to examine effects of materials on the shape of beam. The results are shown in **Figs. 17～21.** These results show similar tendency to AISI 316L stainless steel for the effect of each

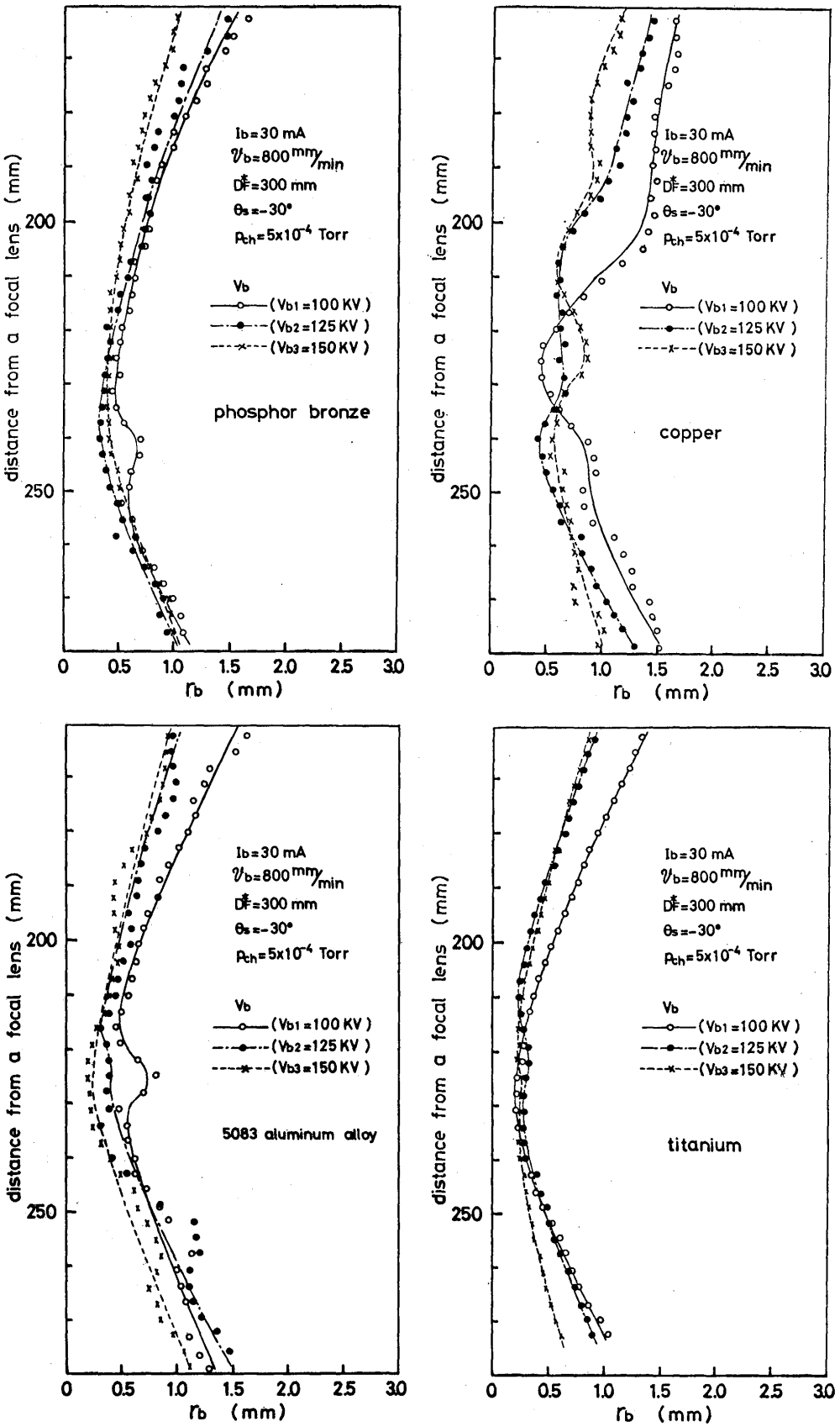

Fig. 17. Relation between beam voltage and beam shape for various materials (A type test).

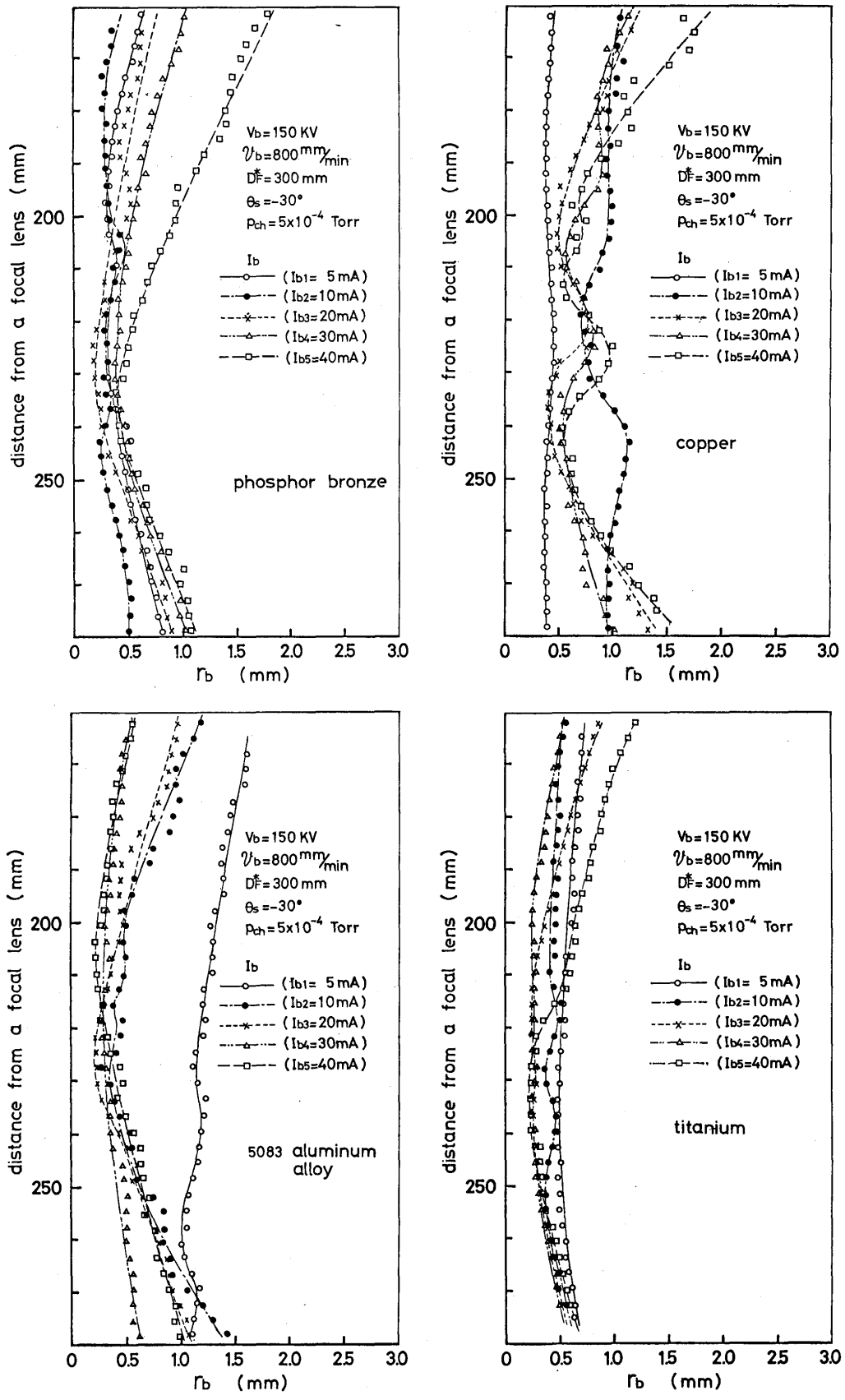

Fig. 18. Relation between beam current and beam shape for various materials (A type test).

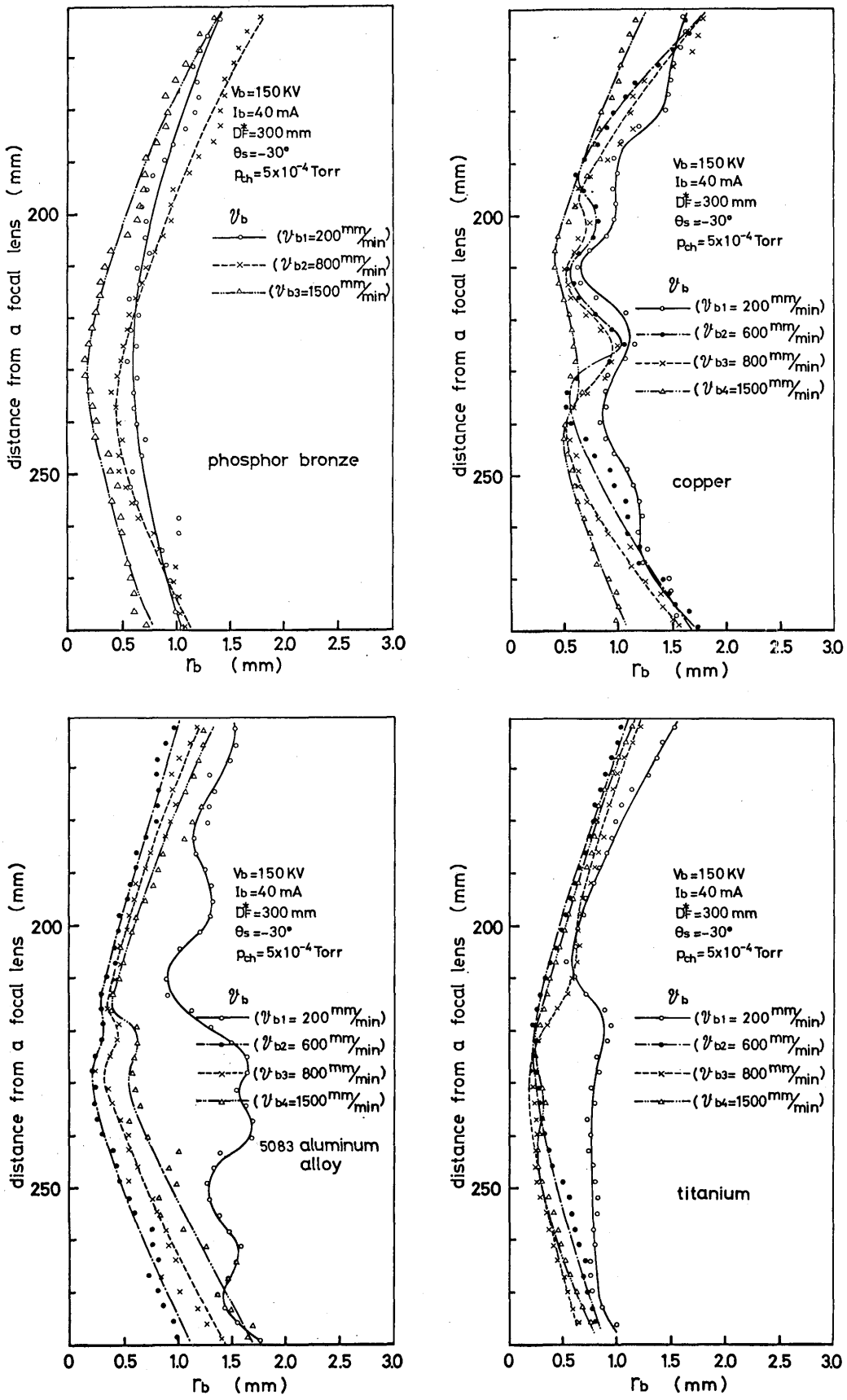

Fig. 19. Relation between welding speed and beam shape for various materials (A type test).

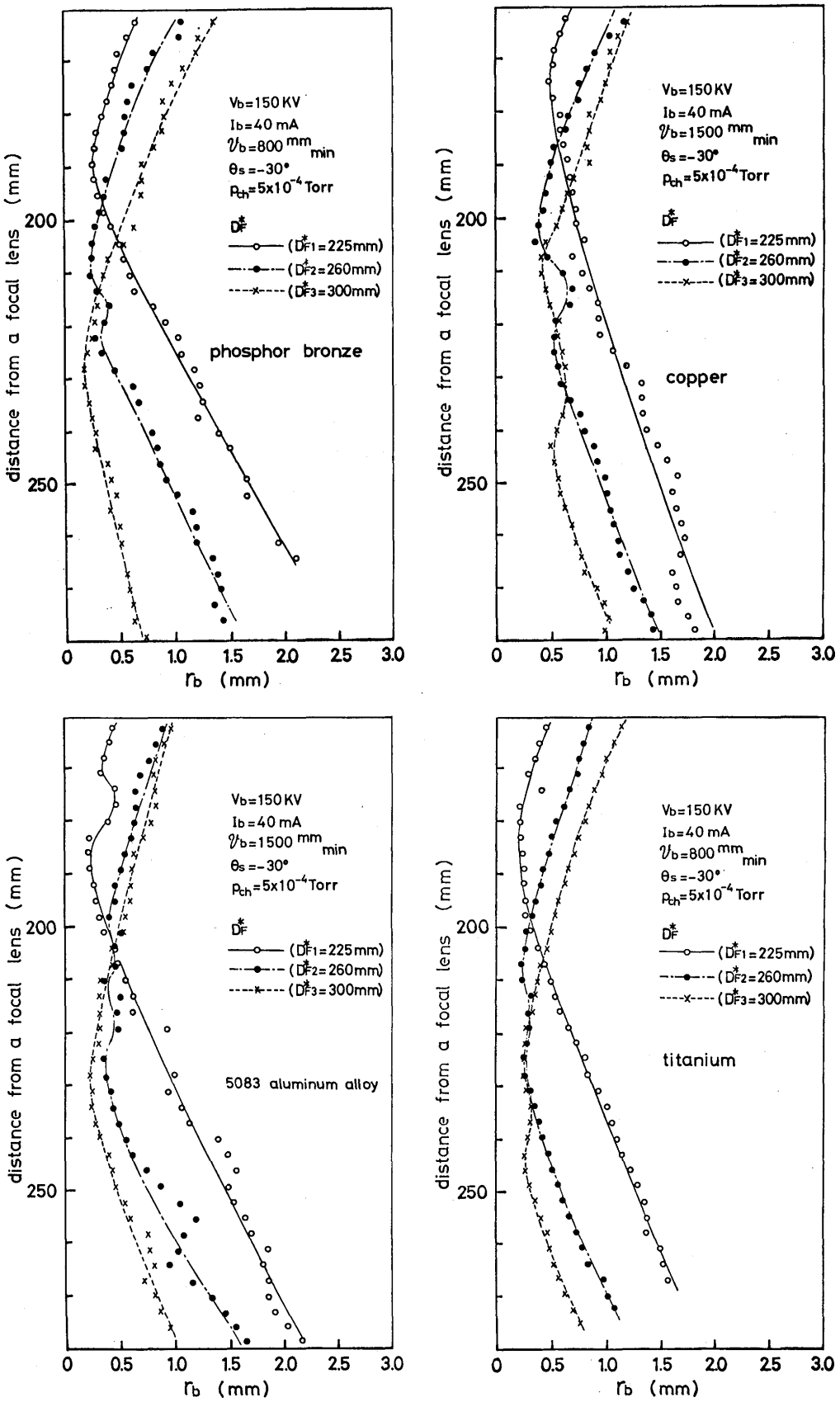

Fig. 20. Relation between visual focal length and beam shape for various materials (A type test).

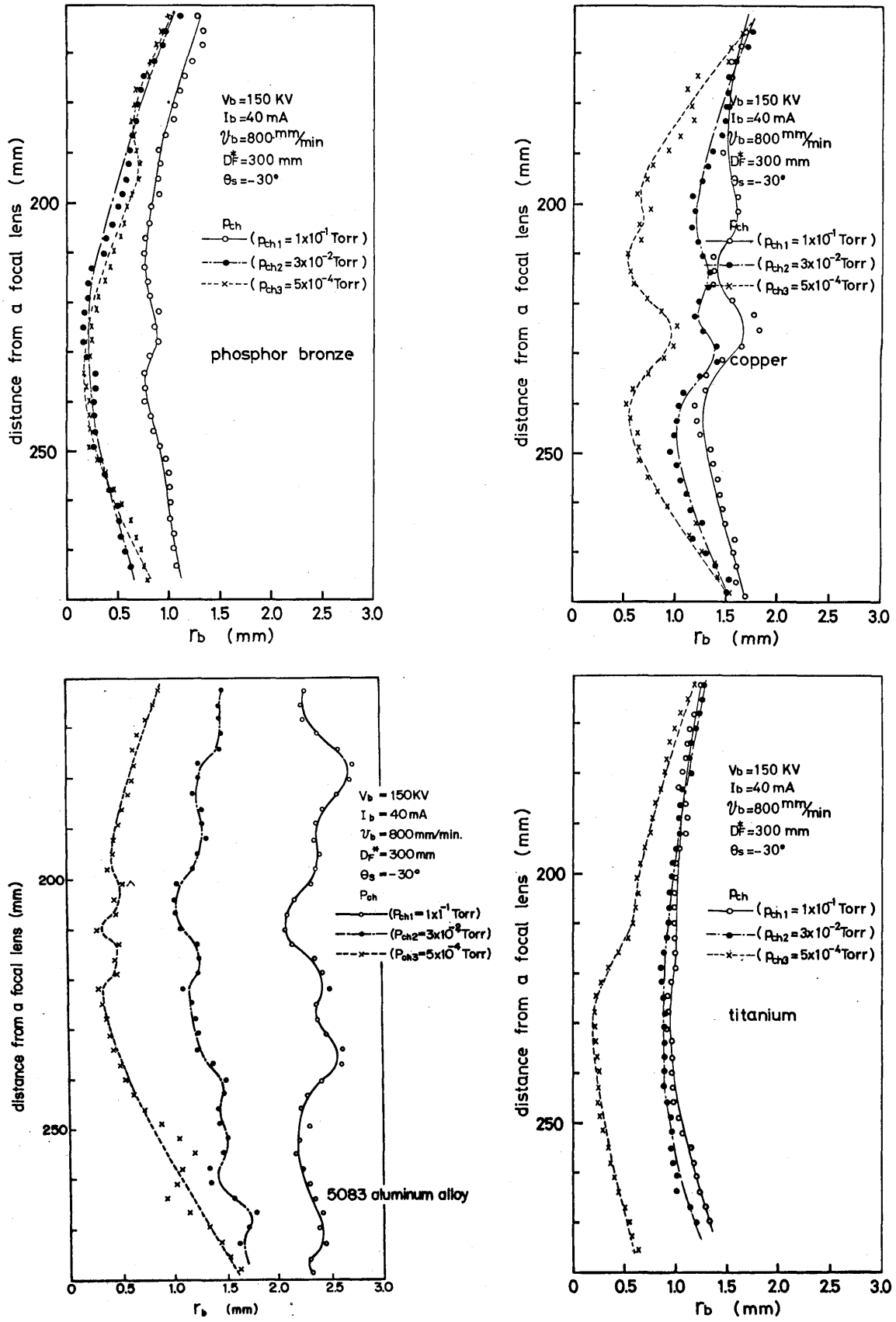

Fig. 21. Relation between gas pressure in vacuum work chamber and beam shape for various materials (A type test).

welding parameter on the shape of beam. As shown in Fig. 19, however, welding speed has a marked effect on the shape of beam for copper and 5083 Al alloy. Particulary, when welding speed becomes slow, secondary melting effect appears as shown in **Photo. 4** so that actual beam diameter is not indicated around the focal point. Also, the result in Fig. 18 shows widened beam diameter in small current range, which may give rise to the beam acted as surface heat source producing slightly melted surface, concerning both effects of large heat conductivity of the material and lower beam power, and molten metal was remained at the edge without burn through as shown in **Photo. 5.**

However, if the limited condition is given to these materials (copper and 5083 Al alloy, etc.), for example, exceedingly fast welding speed with large beam power is used, similar results to those for other materials can be obtained. It has proved, therefore, that measurement of the shape of beam by this method can be applied to any material.

3-3-3 Effects of vaporization on the shape of beam

In order to examine effects of vaporization on the shape of beam, slope welding was performed using 7075 Al alloy in which asily vaporized element (Mg and Zn, etc.) was contained. Effect of gas pressure in vacuum work chamber was examined under the fixed welding conditions ($V_b = 150$ KV, $I_b = 40$ mA, $v_b = 1500$ mm/min, $D^*_F = 300$ mm). The results show, as shown in **Fig. 22,** the similar shape of beam to other materials described above is obtained, and fairly good results are obtained under low vacuum of 10^{-2} Torr. On the contrary, when gas pressure in vacuum work chamber is decreased and vaporization becomes vigorous, they make it impossible to obtain the correct shape of beam. It is natural that such disorder should appear, and determination of gas pressure in vacuum work chamber in consideration of vapor pressure for easily vaporized element contained in the material and beam expansion vacuum is required for a material with remarkable vaporization occurs in the vicinity of focal point. As shown in **Fig. Fig. 23,** when quartz (2 mm$^{(t)}$ × 40 mm$^{(W)}$ × 300 mm$^{(L)}$) which brings extremely vigorous vaporization was used as a test piece, similar beam shape to that of an ordinary metal material was obtained though slightly narrow. It is considered that this result is caused by the effect of space charge which is charged up on the test piece.

To prevent such space charge effect, authors used parallel-arranged ceramic strip fixed by jig of steel, as show in **Fig. 24,** to make space charge

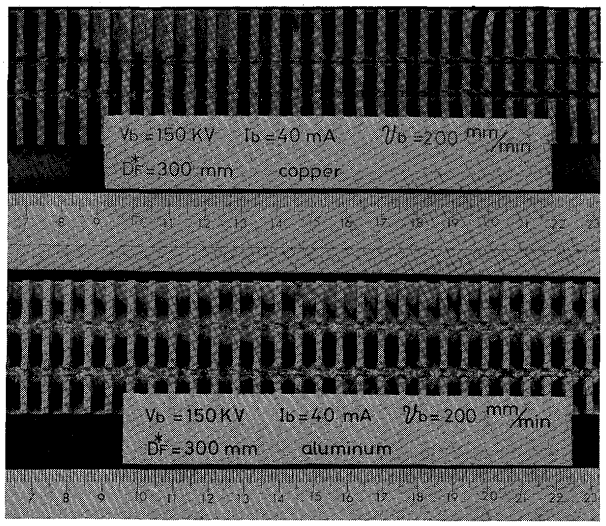

Photo. 4. Swelling of measured beam diameter in the vicinity of focal point.

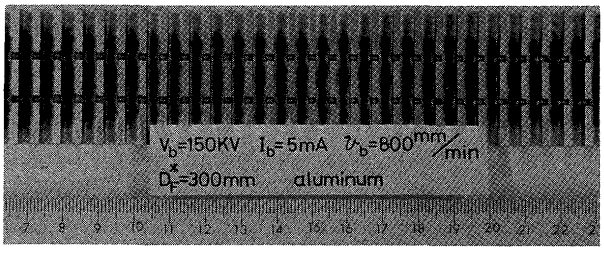

Photo. 5. Bead profile in case of using small beam current.

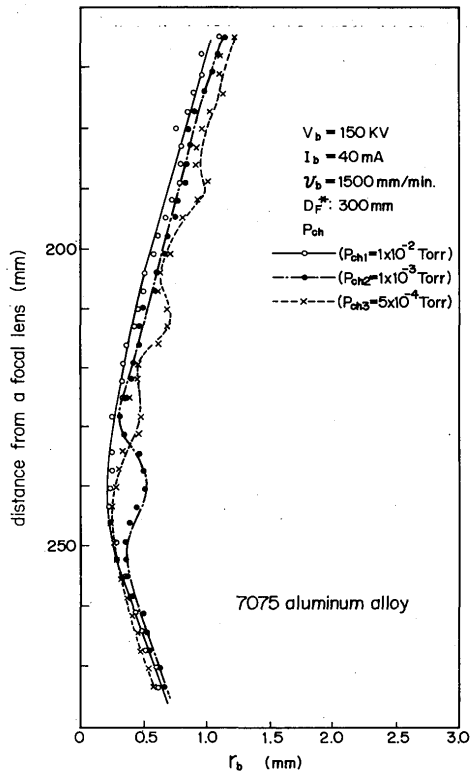

Fig. 22. Relation between gas pressure in vacuum work chamber and beam shape for 7075 aluminum alloy (A type test).

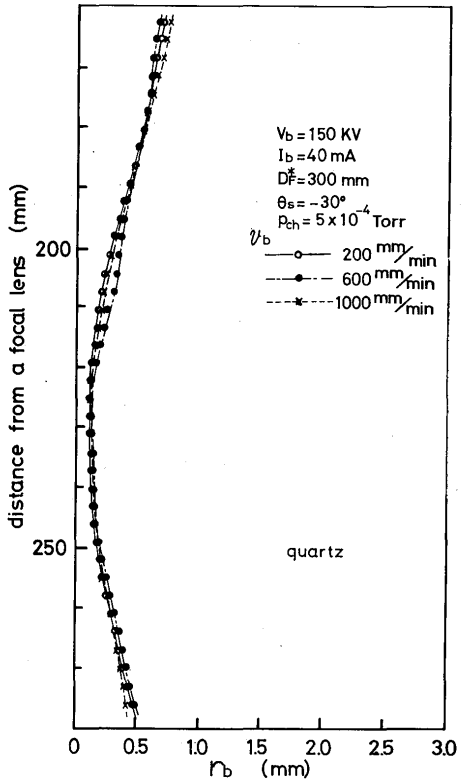

Fig. 23. Relation between welding speed and beam shape for (A type test).

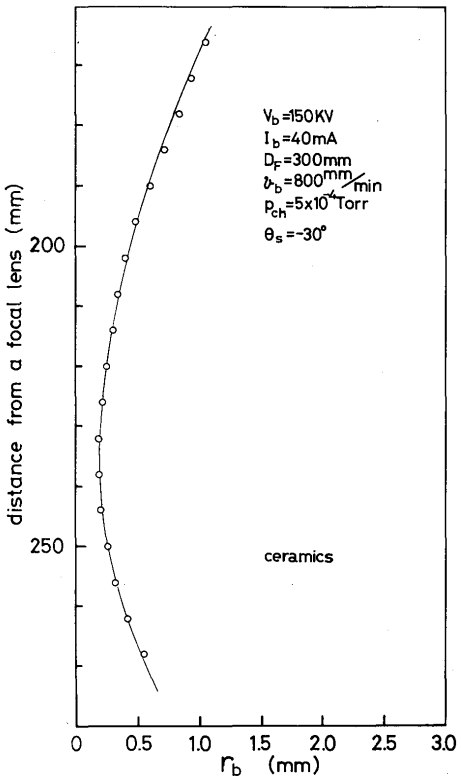

Fig. 25. Beam shape in test piece with parallel-arranged ceramic strip fixed by jig of steel.

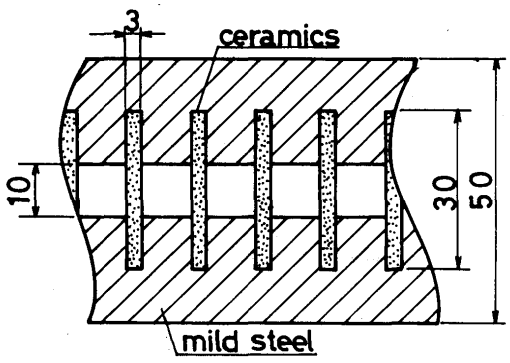

Fig. 24. Schematic drawing of test piece with parallel-arranged cermic strip fired by jig of steel.

escape to the fixed jig of steel through plasma generated around the ceramic specimen. As this result, beam shape is approximately corresponded to the one gained in the specimen of AISI 316L stainless steel as shown in **Fig. 25.**

3-3-4 Tests on reliability of A type testing method

The problems of A type testing method in which downslope welding was used, i. e., effects of flow of molten metal with the test piece placed obliquely on the measured value of beam diameter were examined by using B type testing method ($\theta_s = 0°$) in which glide welding was used as shown in Fig. 5.

As a test piece, AISI 316L stainless steel and titanium, by which relatively smooth beam shape was obtained in A type testing method, were adopted, and the test was conducted under the same conditions as A type. The results are shown in **Figs. 26 ~29,** which agree well with those of A type testing method on the beam shape and minimum beam diameter.

3-3-5 Summary

From the above results, proper beam shape for each type of material is summarized in **Fig. 30.** From Fig. 30, since tendency and minimum beam diameter for each material almost agree except a few materials (Cu and quartz), this measuring method can be applied to any type of material. In the case of Cu, it is considered that the same results can be obtained if the welding is performed with a large beam power at much faster welding speed. It is therefore allowed to use cheaper materials instead of high priced materials used for welding in affirmation of shape of beam and energy density prior to practical welding. The most suitable material of the test piece that can be recommended from such point of view is stainless steel followed by killed steel. Practically speaking, such beam properties (shape of beam, focal point, energy density) vary oftened in accordance with the use of filament and its replacement, so that it is better these should be measured before welding.

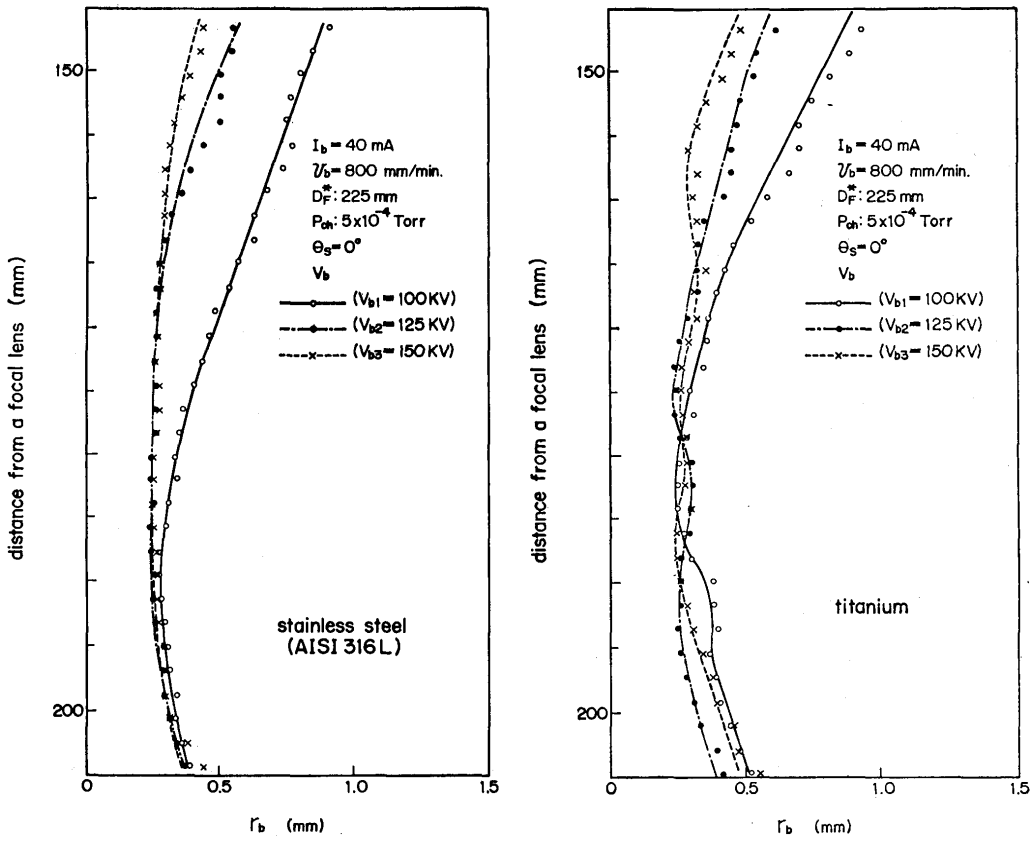

Fig. 26. Relation between beam voltage and beam shape (B type test).

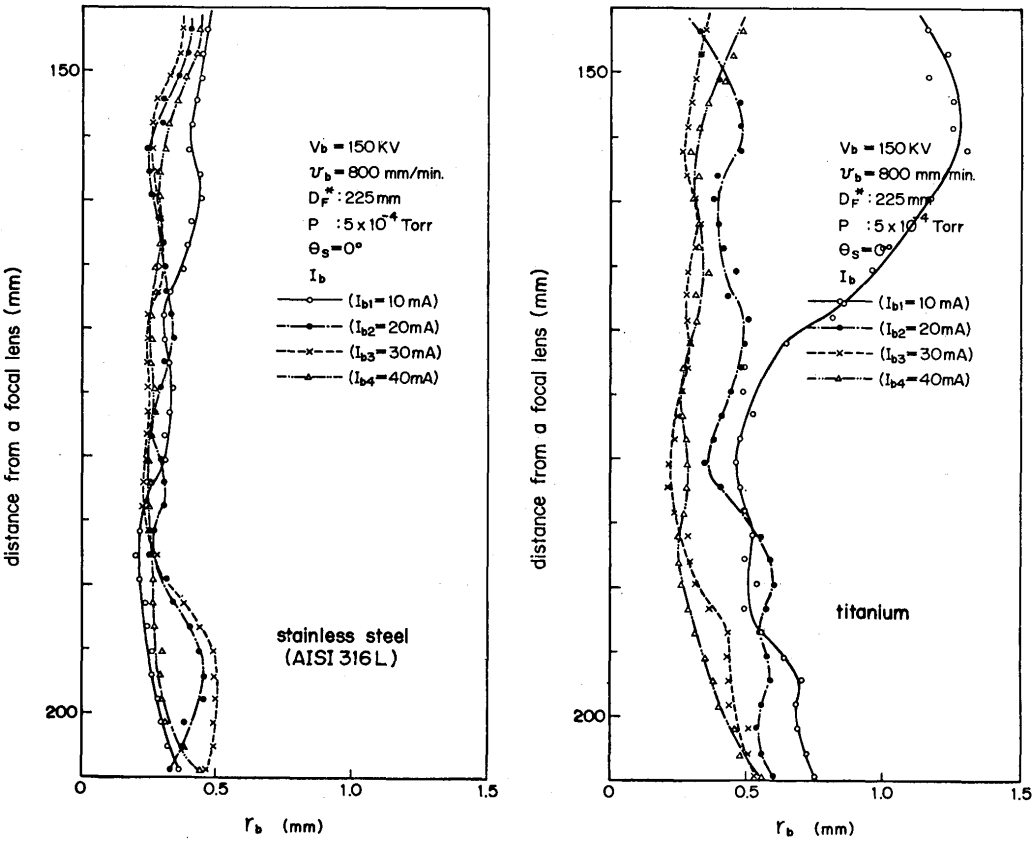

Fig. 27. Relation between beam current and beam shape (B type test).

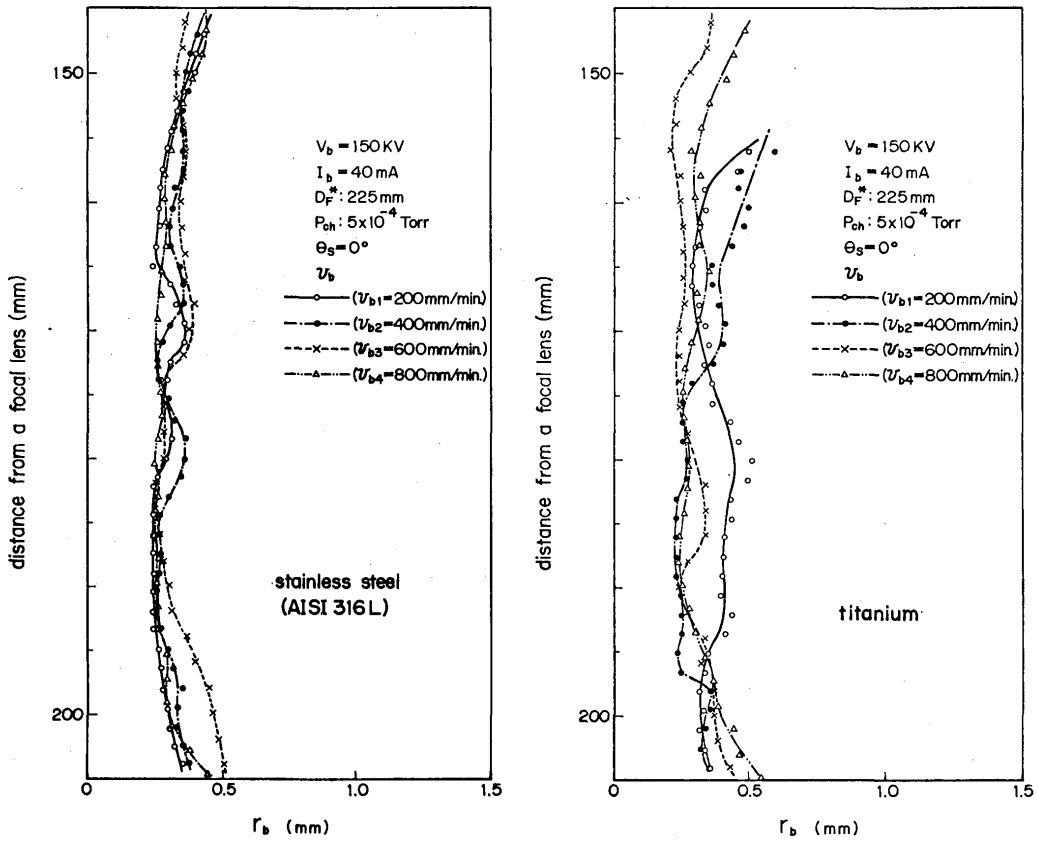

Fig. 29. Relation between gas pressure in vacuum work chamber and beam shape (B type test).

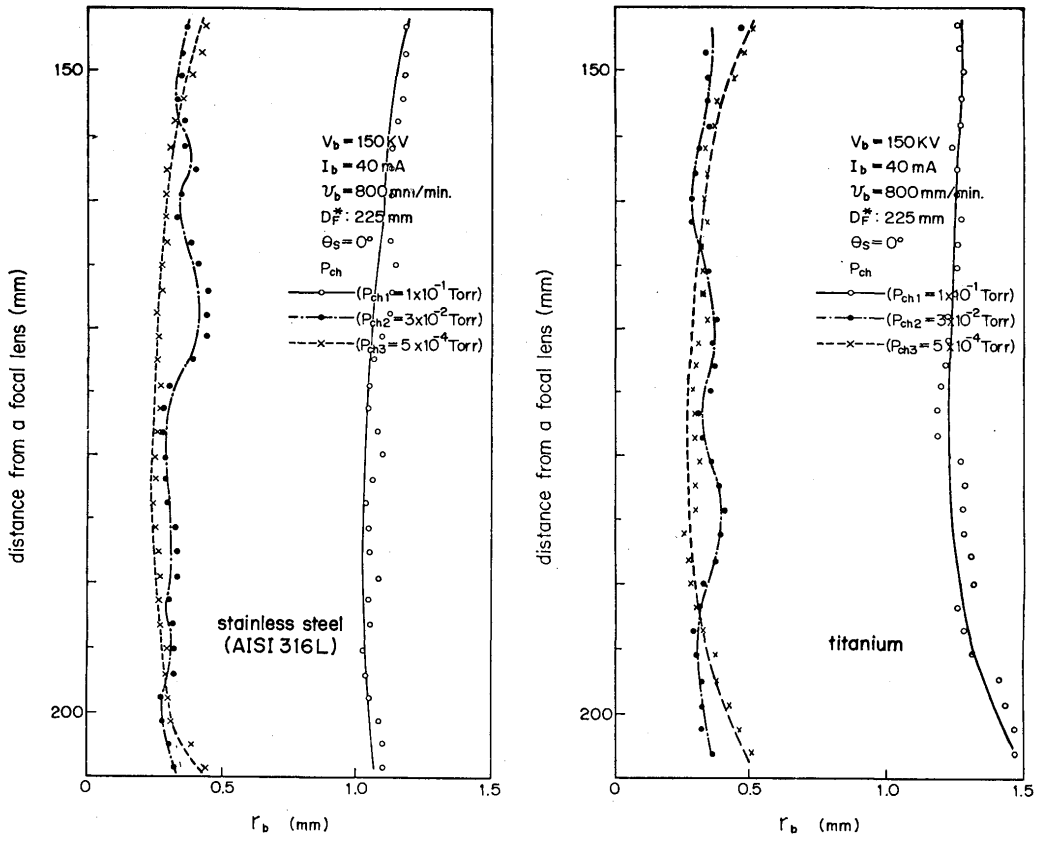

Fig. 28. Relation between welding speed and beam shape (B type test).

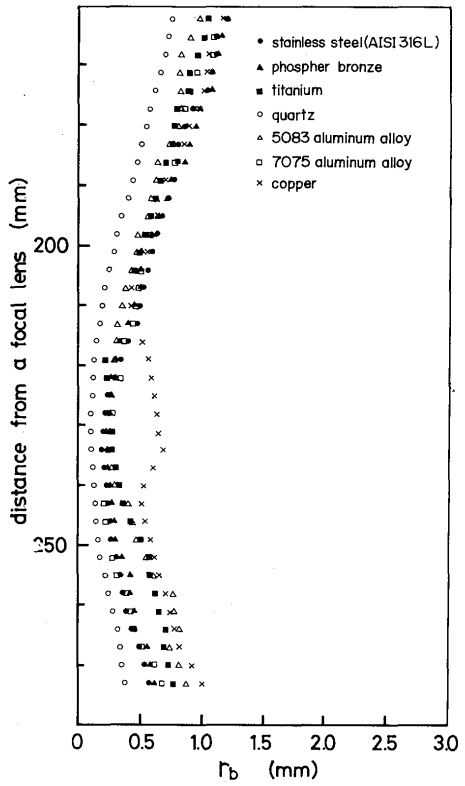

Fig. 30. Summarization of proper beam shape for each type of materials.

4. Conclusion

From the test results described above the following conclusion can be drawn.

1) The new beam test method has been achieved by using 2 types of welding methods ("slope welding", particularly "downslope welding" and "glide welding") and a test piece having function of edge effect.
2) Since this method can be performed under the same conditions as the practical welding, namely, the same beam conditions as during the welding (beam voltage, beam current, shape of beam, welding speed, gas pressure in vacuum chamber and a_b value) and the test piece of the same material as welds can be used, effective beam diameter and energy density during the practical welding can be measured.

   Only the difference between this testing method and the practical welding is that the test piece has function of edge effect.
3) This method allows to observe effective profile at a glance quite easily and correctly: focal point of beam and its effective energy density under any welding condition can be measured correctly.
4) It was proved that, in vacuum range $(0.3-1)\times10^{-1}$ Torr, interaction between electron beam and its beam plasma became vigorous, and energy density abruptly decreased due to abrupt expansion of beam diameter ("beam expansion"). From the above fact, it was also proved that so-called "beam expansion vacuum" exists for powerful electron beam and relation between gas pressure in vacuum work chamber and penetration depth, which was already measured but remained unexplained, could be properly explained.
5) This testing method can be applied to all the weldable materials. Practically, it can be recommended that stainless steel is the best as a test piece followed by killed steel.
6) Welding conditions as a test piece to obtain effective beam diameter for such materials as stainless steel and steel having inferior heat conductivity and good fluid of liquid metal are rather easy in restrictions whereas those for such material having good heat conductivity as Cu and Al or containing a large amount of element of vaporosity with high vapor pressure are severe in restrictions.
7) Remarkable secondary melting phenomenon may appear on some materials under certain welding conditions and burn through effect disappears. In such a case, true beam diameter does not show. On the contrary, such phenomenon will help to study property of the material in high temperature.
8) In an insulating material, beam shape is approximately corresponded to the one with AISI 316L stainless steel by use of parallel-arranged ceramic specimen fixed by jig of steel or other metals.

References

1) Y. Arata: "Characteristics of Electron Beam Heat Souce and View of Development on Electron Beam Welding Technology", J. Japan Welding Society, Vol. 41, No. 11 (1972).
2) Y. Arata, M. Tomie and Y. Katoh: "Some Properties of 30-KW class Electron Beam for Welding", Vol. 2, No. 1 (1973).
3) Y. Arata, K. Terai and S. Matsuda: "Study on Characteristics of Weld Defect and Its Prevention in Electron Beam Welding (Report 1)", Vol. 2, No. 1 (1973).
4) Y. Arata, M. Tomie, K. Terai, H. Nagai and T. Hattori: "Shape Decision of High Energy Density Beam (Report 1)", Document of Committee of Electron Beam Welding, JWS, No. EBW-69-72 (1972).
5) Y. Arata, M. Tomie, K. Terai, H. Nagai and T. Hattori: "Shape Decision of High Energy Density Beam (Report 2)", Document of Committee of Electron Beam Welding, JWS, No. EBW-76-73 (1973).
6) H. Suzuki, T. Hashimoto and F. Matsuda: "Characteristics of Electron-Beam for welding", J. Japan Welding Society, Vol. 32, No. 5 (1963).
7) K. Terai, T. Toyooka and H. Nagai "Effects of Process Parameter on the Penetration Depth in High Voltage Electron Beam Welding", Transaction of Japan Welding Society, Vol. 3, No. 1 (1972).